

Background and Sensitivity Simulation of a Space Based Germanium Compton Telescope

B. L. Graham

George Mason University, Institute for Computational Sciences and Informatics,
4400 University Dr, Fairfax VA 22030-4444

B. F. Philips,

Universities Space Research Association,

J. D. Kurfess and R.A. Kroeger,

Naval Research Laboratory,

Code 7650, 4555 Overlook Ave. SW Washington DC 20375

Abstract—A Monte Carlo simulation code has been developed that calculates the isotopes produced by spallation and propagates the products of radioactive decays for the purpose of studying activation backgrounds in space based gamma-ray telescopes. This code has been applied to study a Compton telescope consisting of two large arrays of position sensitive germanium detectors. Activation of the germanium by cosmic rays and their secondary particles is the major source of background. These simulations quantify the contributions and spectrum of each background component.

I. INTRODUCTION

Improved gamma-ray telescopes with better sensitivity are needed to observe fainter objects of astrophysical significance, to better resolve spatial and spectral features objects already known. The Compton telescope COMPTEL aboard the Gamma Ray Observatory (GRO) demonstrates the utility of a Compton telescope with its wide field of view and sensitivity [1]. A Compton telescope using germanium detectors with greatly improved energy resolution will have much better sensitivity and imaging capabilities. The goal of this work is to quantify the background in a Germanium Compton telescope.

A Monte Carlo model has been used to simulate the efficiency, point spread function and background rate for various configurations of Compton telescopes. The baseline Compton telescope modeled consists of two large arrays of position sensitive germanium detectors. The upper array of detectors is designed to scatter gamma rays and the lower detectors to absorb the scattered photon. The measured positions and energies of the interactions in the two detector planes allow the projection of a ring on the sky indicating possible directions from which the source photon came. The error in the positions and energies determine the width of the ring. The sum of many rings allows for imaging point sources and diffuse sources.

The major background components included in this simulation are the diffuse cosmic gamma-ray flux [2], Earth's atmospheric gamma-ray flux [3], and the decay of nuclei produced by spallation of cosmic rays, trapped protons and their secondary particles. The method for calculating the nuclear activation and decay component of the background combines the particle environment with spallation cross-sections and nuclear decay data. The proton and neutron

environment that activates the instrument is based on the method outlined by Gehrels [4,5], which estimates the primary and secondary protons and neutrons but does not propagate primary proton via Monte Carlo. The spallation cross sections are taken from Alice91 [6] and YieldX [7,8]. The nuclear decay data is taken from the National Nuclear Data Center's (NNDC) Evaluated Nuclear Structure Data File (ENSDF) database [9]. The three-dimensional transport of gamma-rays and β particles was done with Electron Gamma-ray Shower version 4 (EGS4) [10] using MORSE-CG. This Monte Carlo model has been tested by modeling the HEAO 3 gamma-ray instrument background [11,12]. This Monte Carlo code handles the following decay types: electron capture, β^- , β^+ , meta-stable isotopes and short-lived intermediate states, and isotopes that have branchings to both β^- and β^+ . The code generates a cascade of photons to the ground state of the decay product for every decay of an unstable spallation product, and propagates these photons and appropriate accompanying β simultaneously.

II. MODEL

The large space based Compton telescope (proposed as the Advanced Telescope for High Energy Nuclear Astrophysics, ATHENA mission [13]) used in this simulation consists of germanium detectors, aluminum cryostats, aluminum support structures and an aluminum spacecraft.

The germanium detectors are modeled as two solid parallel planes with a total area of 1 m^2 . The upper detector (D1) is 2 cm thick and the lower detector (D2) is 6 cm thick. The two detector arrays are separated by 100 cm. The detectors are segmented into 2 mm by 2 mm by 1 cm pixels with an energy resolution of 2 keV FWHM [14,15]. This energy resolution is comparable to the performance these detectors have achieved in the laboratory with the current generation of Application Specific Integrated Circuits (ASIC) [16]. The threshold used for the upper detectors was 20 keV. The threshold used for the lower detector was 40 keV. The threshold used for total energy was 300 keV.

The aluminum cryostats that surround each detector array are 2 mm thick with a total mass of nearly 30 kg for each cryostat. The spacecraft was modeled as a solid component of aluminum located below the lower detector (D2) with a mass of nearly 300 kg.

III. SIMULATION

The simulations were done using Monte Carlo transport code EGS4 for propagating photons and β particles to simulate point sources, diffuse sources and the decay of unstable isotopes.

The efficiency and angular resolution of the telescope was modeled for a point source. A point source was Monte Carlo modeled by fully illuminating the area of the upper detector with mono-energetic beams of gamma rays. These beams were at normal incidence and a variety of energies was used from 300 keV to 10 MeV.

The point spread functions were calculated for several energies using a ring sum image reconstruction technique. Screening, as discussed in the next section, was applied to the data set for several energies. The data is screened and converted to the Compton scattering phase space of scatter angle, error in scatter angle, and scatter direction. A normalized event ring sum is used to generate an image of the point source on a very fine grid. The normalized event ring sum is calculated by projecting each coincidence event as a ring onto the sky and assigning a value to each sky pixel so that the total value each ring contributes is one. The angular resolution for a point spread function is shown in Figure 1b as the angular extent of the reconstructed image of a point source that is within 1σ of the maximum intensity. The efficiency, shown in Figure 1a, was determined from the rings that reconstruct to intersect within this angular resolution of the point source.

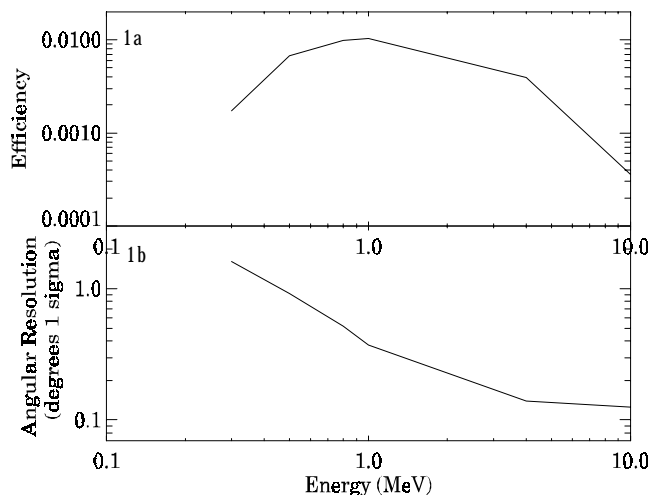


Figure 1a. Normal incidence Efficiency. Figure 1b. Angular resolution (1σ)

The diffuse sky was simulated by modeling the response to isotropic diffuse gamma rays and convolving that response with the cosmic diffuse gamma-ray flux. The response to isotropic gamma rays was modeled by illuminating the

instrument with mono-energetic gamma rays isotropically at a variety of energies. Then the photo-peak efficiency and efficiency for partial energy absorption were determined after screening and reconstruction were applied (as discussed in the next section). The efficiency to isotropic diffuse gamma-rays is 4.0×10^{-4} coincidences per incidence gamma-ray for the photo peak at 1 MeV and 2.7×10^{-4} coincidences per incidence gamma-ray for all 1 MeV gamma-rays that are partially absorbed and contribute to the continuum. The entire response matrix is filled by interpolating along the diagonals between the energies modeled.

The background spectrum from the Earth's atmospheric flux was calculated by folding the atmospheric gamma-ray flux through the diffuse response. Then the spectrum was scaled by the solid angle subtended by the Earth. The spectrum is also scaled for when the instrument is turned off when the center of the Earth is within 45 degrees of the center of the field of view. This is done to the spacecraft being three axes stabilized and being pointed at a source at all times.

The activation background was modeled for each component of the instrument according to the method outlined in Graham et al. [12]. For each component of the instrument, radioactive decays of unstable isotopes were modeled for all unstable isotopes with production $>0.1\%$ of the most abundantly produced isotope by spallation. The particle environment was estimated for a 5 degree, 400 km Low Earth Orbit (LEO). The proton and neutron environment LEO is estimated according to the method used by Gehrels [4] (which includes an approximation for primary and secondary particles). The prompt signals (from primary protons) are assumed to be vetoed.

IV. SCREENING

Four important methods of data screening were used: veto of multiple signals in D1, time of flight, reconstruction of path of the incident gamma-ray in D2 and phase space screening.

First, valid events are coincidences for where the incident gamma-ray interacts only once in D1 and multiple interactions are allowed in D2. The screening of multiple signals in D1 also helps with background rejection, by removing decays that emit multiple gamma rays. Events that interact in multiple locations in D1 cannot be imaged and are therefore rejected.

COMPTEL has the capability to measure the time for a gamma-ray to travel between scatters in D1 and D2; this is called the time of flight measurement. Time of flight permits upward moving gamma-rays to be discriminated from downward moving gamma-rays.

Since an energetic incident photon may scatter several times in D2 before it is absorbed, multiple signals per coincidence are allowed in D2. When a gamma-ray scatters several times in D2 generating signals in multiple pixels, the path of the gamma-ray is deduced to determine the first

interaction in a pixel in D2. The Compton scatter formula is applied. This reconstruction is done by comparing the difference between the scatter angle calculated using position of the interaction and the scatter angle calculated by the energy in the pixels. The pair of signals with the minimum difference is accepted as the path of the first scatter in D2. Events are rejected in this analysis when the first pixel cannot be determined with an acceptable probability. Events interacting in neighboring pixels only are generally rejected.

Finally, screening in the Compton scattering phase space (scatter angle and scatter direction) is done to eliminate coincidence events, which have a total scatter angle and scatter direction of greater than 90 degrees off axis. This was used initially because objects that were to be observed are in front of the instrument and objects that are sources of background (the spacecraft, earth) are to the rear. This is a good method for background rejection for activation in D1, due to events leaving most of their energy in D1 and only a little in D2, therefore reconstructing to large scatter angles

V. RESULTS

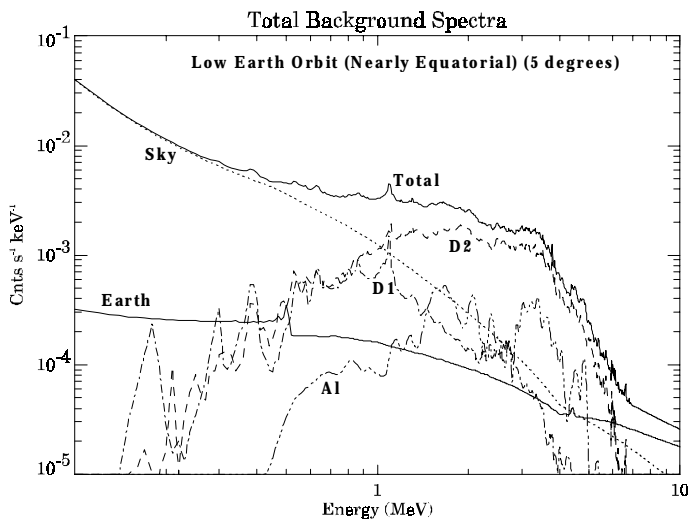


Figure 2. Components of the background spectrum. The dashed and dotted curve is the background spectrum due to coincidences from activation in D1. The dashed curve is background spectrum due to coincidences from activation in D2. The dotted curve is the background response from the cosmic diffuse gamma rays. The dashed and triple dotted curve is the background spectrum from activation in all of the aluminum components. The solid curve is the background spectrum from atmospheric gamma rays. The thick solid curve is the sum of all these components.

The components of the background spectra are shown in Figure 2 for LEO for the case of no time of flight background rejection. The total background spectrum is dominated by the activation in both detectors. There is a significant contribution from the aluminum activation. The cosmic diffuse emission dominates at low energies. The atmospheric gamma ray flux dominates the background at high energies.

The total background count rate is 3.3×10^{-3} counts $s^{-1} keV^{-1}$ at 1 MeV.

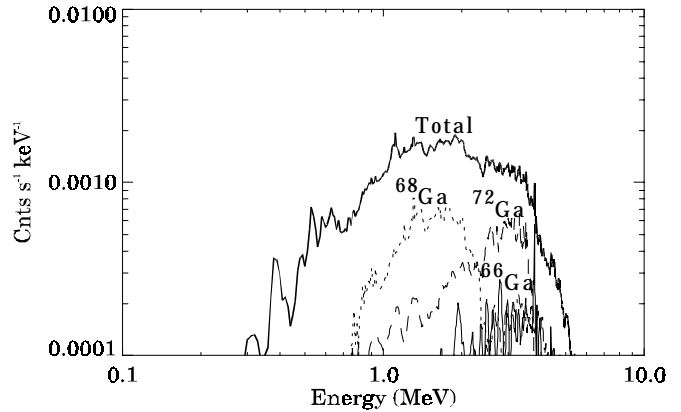


Figure 3. The three largest components of the background from decays in D2 and the total background spectrum from decays in D2. The largest three components are decays from ^{66}Ga (Solid), ^{68}Ga (dotted) and ^{72}Ga (dashed).

Figure 3 shows the three isotopes that are the largest contributors to the background from decays from activation in D2. These are Ga^{66} , Ga^{68} and Ga^{72} . The total background is also shown in Figure 3 from activation in D2 from all unstable isotopes with production $>0.1\%$ of the most abundantly produced.

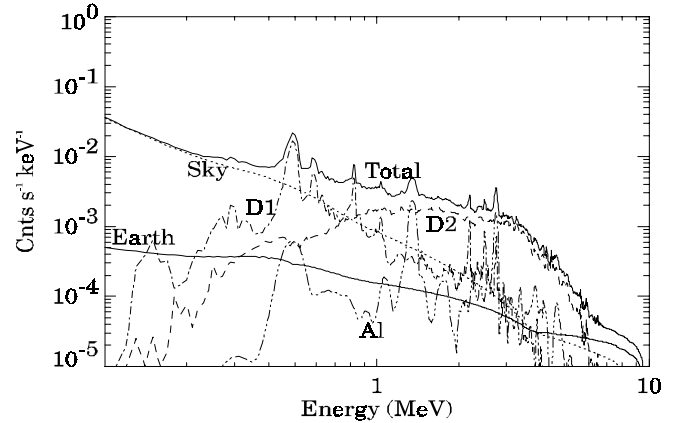


Figure 5. A spectrum of the signals of the background coincidences in D2. The dashed line is the contribution from decays in D2. The dashed and dotted curve is the contribution from decays in D1. The solid curve is the contribution from atmospheric gamma-rays. The dotted curve is the contribution from diffuse cosmic gamma-rays. The dashed and triple dotted curve is for decays from the aluminum components.

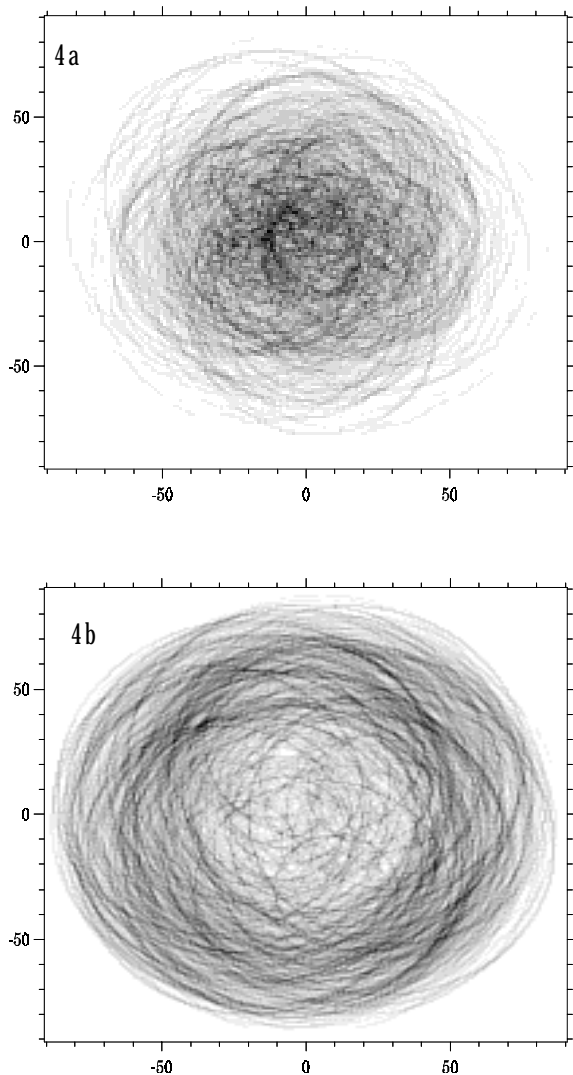


Figure 4a. Reconstructed image of background from ^{69}Ge decay in D2 at 1 MeV. Figure 4b. Reconstructed image of background from ^{69}Ge decay in D1 at 1 MeV.

Decays of ^{69}Ge were reconstructed and imaged to show the distribution of the background on the sky. Figure 4a shows the reconstructed image of the distribution of the background of ^{69}Ge at 1 MeV (for decays of ^{69}Ge in D2 figure 4a and for decays of ^{69}Ge in D1 figure 4b). The distribution peaks away from the center of the field of view for decays in D1 of ^{69}Ge at 1 MeV. The distribution peaks at the center of the field of view for decays in D2 of ^{69}Ge at 1 MeV.

Figure 5 shows the total spectrum of signals in D2. From decays in D1, there are lines in this spectrum at 0.548 MeV and 0.637 MeV, which come from the decay of ^{62}Zn . There are lines at 2.752 MeV and 1.039 MeV from the decay of ^{66}Ga . There are strong lines from the decay of ^{24}Na at 1.368 MeV and 2.754 MeV. There are also lines at 0.834, 2.201, and 2.507 MeV from the decay of ^{72}Ga . The elimination of the strongest of these lines can be used to reduce background,

improving sensitivity, for lines that reduce more background than source efficiency.

VI. DISCUSSION

The spectra in Figure 2 shows the background rate is dominated by activation in the lower detector at 1 MeV. The background in this Compton telescope has a significant β continuum shape. This is primarily a result of a major portion of the background coming from coincidences between a β particle in one detector and a gamma ray in the other detector.

The model for the background spectrum is limited by the detail of the mass model, the particle environment, and the spallation cross-sections. The mass model does not include passive detector material between the detectors that comprise each detector plane or gaps between these detectors. Including the passive material for each detector could increase the background by as much as 20%. The proton and neutron environment used from Gehrels [3,4] may not be appropriate because the estimation for secondary particles is determined through a thick shield. The decay of unstable decay products was not modeled. Including the decay of unstable decay products could increase the production and decay rates of some isotopes by a few percent. The Alice91 cross-sections have a reported error of 30%.

Achieving the capability of time of flight in the germanium Compton telescope can significantly reduce the background component from decays in D2. If one assumes that the time of flight capability eliminate the entire contribution from decays in D2 then the total background rate becomes 2.0×10^{-3} counts s^{-1} keV^{-1} at 1 MeV. While useful, time of flight is not essential in a germanium Compton telescopes.

Coincident inelastic neutron scatters are not modeled. The resultant background component can be calculated from the convolution of steep neutron spectra. This component will primarily effect the background at low energies. Time of flight can be used to determine slow neutrons from gamma-rays, thus eliminating the contribution from coincident inelastic scatters of neutrons.

The gamma-ray lines at 0.548 MeV, 0.637 MeV, 0.834 MeV, and 1.039 MeV energies can be seen in the lower detector from decays in the upper detector, as shown in Figure 5. These lines and others can be used to identify and eliminate background. These lines are produced from decays with a β in D1 and a gamma-ray fully absorbed in D2. Depending of the intensity of the line, vetoing these lines in a detector may reduce the background more than the reduction in the efficiency, thus improving sensitivity

Energetic incident photons may scatter several times in D2 before being absorbed. Thus, multiple signals per coincident event are allowed in D2. The integrated background rate for decays in D1 is 0.08 counts s^{-1} . The integrated background rate for decays in D2 is 0.46 counts s^{-1} . The ratio of the integrated background rates should be a

factor of three because D2 is three times the volume of D1. The ratio of background events due to decays in D2 and D1 is larger than the ratio of the volumes because decays with multiple interactions in D1 are vetoed.

The sensitivity for ATHENA shown by Johnson et al. [12] was based on an instrument background of the diffuse sky scaled by a factor of 4 to account for the activation component of the background. This approximation underestimated the background above 1 MeV where the activation component is the strongest. The total background based on an improved treatment of the ambient proton and neutron environment is needed to further refine these calculations.

REFERENCES

- [1] V. Schönfelder et al., "Instrument description and performance of the imaging gamma ray telescope COMPTEL aboard the Compton gamma-ray observatory," *Ap. J. S.*, Vol 86, pp. 657, 1993.
- [2] R. Kinzer et al., "Diffuse cosmic gamma radiation measured by HEAO 1," *Ap J.*, Vol 475, pp. 361-372, 1997.
- [3] J. Letaw et al., "Satellite observation of atmospheric nuclear gamma radiation," *J. Geophys. Res.*, Vol. 94, pp. 1227, 1989.
- [4] N. Gehrels, "Instrumental background in balloon-borne gamma ray spectrometers and techniques for its reduction," *NIM A*, Vol. 239, pp. 324, 1985.
- [5] N. Gehrels, "Instrument background in gamma ray spectrometers flown in low Earth orbit", *NIM A*, Vol. 313, pp. 513, 1992.
- [6] M. Blann and H. Vonach, "Global test of modified precompound decay models," *Phys. Rev. C.*, Vol. 28, p 1475, (1983).
- [7] C. Tsao and R. Silberberg, "Partial cross-sections in high-energy nuclear reactions, and astrophysical applications. I. Targets with $Z \leq 28$." *Ap.J.S.*, Vol. 25, pp. 315, (1972).
- [8] C. Tsao and R. Silberberg, "Partial cross-sections in high-energy nuclear reactions, and astrophysical applications. II. Targets heavier than nickel." *Ap. J.S.*, Vol. 25, pp. 335, (1972).
- [9] NNDC, National Nuclear Data Center, Brookhaven National Laboratory, Brookhaven, NY.
- [10] W. Nelson et al., "The EGS4 code system," *SLAC-report-265*, Stanford University, 1985.
- [11] B. Graham et al., "Simulation of HEAO 3 background," Proceedings of the 4th Compton Symposium, AIP Press Conference Proceedings 410, 1997. In press.
- [12] B. Graham et al., "Simulation of HEAO 3 background," Proceedings of the 2nd Conference on High Energy Background Radiation in Space, IEEE Press, 1997. In press.
- [13] W. Johnson et al., "Advanced telescope for high energy nuclear astrophysics (ATHENA)," *SPIE Proceedings Vol. 2518*, 1995.
- [14] R. Kroeger et al., "Spatial and spectral resolution of a germanium strip detector," *Imaging in High Energy Astronomy*, L. Bassani and G. di Cocco (eds.), pp. 325-328, 1995.
- [15] R. Kroeger et al., "Spatial and spectral resolution of a germanium strip detector", *SPIE Proceedings Vol. 2518*, pp. 236, 1995.
- [16] R. Kroeger et al., "Charge sensitive preamplifier and pulse shaper using CMOS process for germanium spectroscopy," *IEEE Trans. on Nuclear Science*, Vol. 42, pp. 921-924, 1995.